J. Surface Sci. Technol., Vol 29, No. 3-4, pp. 1-14, 2013

Effect of Ag-N co-doping in Nanosize TiO_2 on Photocatalytic Degradation of Methyl Orange Dye

KIROS GUESH, ABI TADDESSE and O. P. YADAV*

Chemistry Department, Haramaya University, Dire Dawa, Post Box-138, Ethiopia

Abstract — Synergetically modified nanosize TiO_2 semiconductor heterogeneous photocatalyst powder has been synthesized from $TiCl_4$ precursor for producing efficient photocatalyst that may work under visible radiation. The crystallite phase and size of the as-synthesized photo-catalyst were determined by X-ray diffraction (XRD) technique. As-synthesized TiO_2 was found to be nano-crystalline anatase. The absorption edge of the photo-catalyst was evaluated from the UV/ Visible diffuse absorbance spectra. The band gap energies (E_{bg}) of undoped-, Ag-doped-, N-doped- and Ag-N co-doped TiO_2 semiconductor photo-catalysts were found to be 3.14, 3.02, 2.56 and 2.45 eV, respectively. Co-doping of Ag and N in TiO_2 has shown synergetic effect towards photo-catalytic degradation of methyl orange in aqueous solutions. Using Ag-N co-doped TiO_2 photo-catalyst, degradation of methyl orange under UV and visible irradiations were 79.1% and 73.5%, respectively.

Keywords : *Absorbance, degradation, diffraction, nanoparticles, photo-catalyst.*

INTRODUCTION

Dyes released from several chemical industries as a waste material contaminate soils and surface water. These chemicals are carcinogenics and exhibit high toxicity and/ or mutagenicity for several living organisms either directly or through some of their metabolites [1]. Environmental research has paid special attention to dyes because of their being extensive environmental contaminants. For the treatment of pollutants-contaminated water, most of the studies have been focused on the bio-degradation processes [2], chemical oxidation [3], physico-chemical techniques [4] and adsorption

*Corresponding author. E-mail : yadavop02@yahoo.com, Mobile : 00251915021008

methods [5–7]. These methods are either costlier or are unable to convert the pollutants into non-toxic product/s. For example, treatment methods such as adsorption by activated carbon merely concentrate the pollutant chemicals by transferring them to the adsorbent and require secondary treatment for their disposal.

Transformation of pollutants to non-toxic product/s by semiconductor photocatalysis has attracted much attention [8–12]. Photocatalytic degradation of pollutants by semiconductor "photocatalysis" is a novel method for the treatment of polluted water. This process involves both heterogeneous catalysis as well as solar technology. During photo-catalytic process the pollutant compounds break down into carbon dioxide, water and simple non-toxic molecules. Further, in the photocatalytic degradation process, secondary treatment for disposal is not required. The initial step in photocatalysis is the absorption of photons of suitable wavelength adequate to match energy levels of the photoactive material. In case of semiconductors, illumination induces electron promotion from their valence band (VB) to the conduction band (CB) if the energy of the photons exceeds their band width. This process leaves an unoccupied state or 'hole' in the valence band. Most of these electron–hole pairs recombine, releasing the absorbed energy as light or, more frequently, as heat. However, a small percentage of these carriers migrate to the surface where they can be captured by adsorbed molecules to start the catalytic cycle. Ideally, a photocatalyst should be a solid semiconductor which is (i) able to absorb visible and/or UV light, (ii) chemically and biologically inert and photostable, (iii) inexpensive and (iv) nontoxic. Titanium dioxide (TiO_2) is the most used photocatalytic material as it fulfils all of these requirements and exhibits adequate photo conversion values [9,11,13]. TiO_2 has a great number of technological applications such as in pigments, sensors, photovoltaic cells, catalysis, hydrogen production, and as environmental depollutant acting as water disinfectant [14,15] and self cleaning as well as anti fogging agent. It can also be used for recovery of trace metals from water [9,16] and destruction of organic compounds [8,10]. Due to its non-toxic nature, TiO_2 is being used in several everyday products such as : food colorant, toothpaste, pill coatings and chewing gum [17].

Although TiO_2 semiconductor has diverse applications, yet its wide band gap energy (3.2 eV) with low photoactivity in the visible light is the major drawback that limits its use as photocatalyst in a solar-driven system. This is because TiO_2 absorbs in UV region and is, therefore, sensitive only to 4% of the solar light. Although, recently, there has been an intense research interest to improve the photocatalytic efficiency of TiO_2 by altering its morphology (by increasing its specific surface area and porosity), by metal/nonmetal doping and coupling with other semiconductors, yet

the progress is only limited in this direction. The synergetic effect of metal and nonmetal dopants in TiO_2 semiconductor may enhance its absorption edge towards the visible region by lowering its band gap energy and thus may increase its photocatalytic efficiency. The present work reports synthesis and characterization of silver and nitrogen co-doped nanosized TiO_2. The as-synthesized semiconductor nanomaterial has been used to investigate the impact of Ag-N co-doping on the catalytic efficiency of the photocatalyst for the methyl orange dye.

EXPERIMENTAL

Materials :

$TiCl_4$ (MW 189.679 g/mol; Density : 1.73 g/cm³; SD fine chemicals), TiO_2 (Degussa p-25, Germany), Urea (BLULUX), Methyl Orange (Berckland Scientific Supplies), Ammonium Hydroxide (Abron Chemicals) and Silver Nitrate (BLULUX) were of analytical grade and were used as such.

Methods :

Preparation of TiO_2 — 121.1 g of $TiCl_4$ (98%) was added into 500 ml of de-ionized ice cooled water. The solution was stirred vigorously for 30 minutes. To this 26.7 g NH_3 was added, drop-wise, with simultaneous stirring. The precipitate thus obtained was washed repeatedly until no chloride is detected in the filtrate. The precipitate was recovered by centrifugation, dried in an oven at 200°C for 3 hours, calcined at 400°C, cooled to room temperature and stored in a moisture-free atmosphere.

Preparation of Ag-doped TiO_2 — 10 g of as-synthesized TiO_2 (Section 2.2.1) and 10 ml of 34.34 g/L $AgNO_3$ aqueous solution were taken in a ceramic crucible. The mixture was well agitated with glass rod and the solvent (water) was evaporated in an oven at 110°C. The dried powder was calcined in a furnace at 400°C for four hours and then cooled to room temperature.

Preparation of N- doped TiO_2 — 20 gm. of the as-synthesized TiO_2 (Section 2.2.1) and 60 g of urea were mixed well in an agate mortar. The mixture was transferred into a ceramic crucible and calcined at 400°C for four hrs and then cooled.

Preparation of Ag - N co-doped TiO_2 — A 10 g of the as- synthesized N- doped TiO_2 (Section 3.2.3) was mixed with 10 ml 0.2018 M $AgNO_3$ aqueous solution in a crucible. The liquid was evaporated at 110°C and the dried powder was calcined in a furnace at 400^0C for 4 hours and cooled to room temperature.

CHARACTERIZATION

XRD study :

For determining the crystallite structure and size of as-synthesized photocatalysts powders, their X-ray diffraction (XRD) patterns were obtained using a diffractometer (BRUKER D8 Advanced XRD, AXS GmbH,Karisruhe, West Germany) equipped with a Cu target Kα radiation $\lambda = 1.5405\ A^0$) source. The measurements were made at room temperature using accelerating voltage and the applied current as 40 kV and 30 mA, respectively, and scan rate 0.02° per second over 2θ range 4^0 –64°. The obtained XRD pattern was analyzed using DIFFPLUS, Eva, version 6.0 software.

TEM Analysis :

Transmission electron microscopic (TEM) image of photo-catalyst sample was obtained at SAIF Panjab University, Chandigarh, using accelerating voltage 80 KV and magnification 200000x. The photocatalyst powder was dispersed in acetone by stirring in a tank for 15 minutes. A drop of the suspension thus obtained was mounted on a carbon-coated copper grid; the solvent was allowed to evaporate before XRD analysis.

Spectrophotometric measurements :

For determining absorption edge and the band gap energy (E_{bg}) of the synthesized photo-catalysts, their diffuse absorption spectra were obtained using UV-Visible spectrophotometer (Perkin Elmer : model Lambda 950) over the wavelength range : 200–800 nm.

Photo-catalytic degradation study :

Photo-catalytic degradation of methyl orange(MO) was carried out in a reactor consisting of a glass tube with an inlet tube for air purging through the dye solution and an outlet for the collection of samples from the reactor at different time intervals. A 0.5 gm of as-synthesized photo-catalyst powder was added to 250 ml aqueous 100 mg/L methyl orange solution taken in the reactor tube and the suspension was stirred in dark for 60 minutes to attain adsorption/desorption equilibrium before starting irradiation of dye sample in the reactor. During irradiation of the samples by UV or Visible radiation, air was purged into the dye solution. Kept at room temperature. At 20 minutes interval, 10 ml of the reaction mixture was withdrawn and the suspension was centrifuged at 3000 rpm for 15 minutes. The supernant liquid was then filtered through whatmann No. 1 paper. Absorption of the clear filtrate was measured at 450 nm using UV/Visible spectrophotometer (Model : SP65). The concentration of dye in a solution was calculated by comparing the observed

absorbance on the standard linear plot between the absorbance versus concentration of dye.

RESULTS AND DISCUSSIONS

XRD Analysis :

X-ray powder diffraction of as-synthesized photo-catalyst samples are presented in Fig. 1. The observed diffraction peaks in the XRD of TiO_2 (calcined) at : $2\theta = 25.0$, 38.2, 48.0, 53.9, 62.4 and 68.6 corresponding to lattice planes : (101), (004), (200), (106), (215) and (110) reveals the existence of anatase phase of TiO_2 and no traces of brookite or rutile phases were indicated. Further, no additional diffraction peaks in the Ag and/or N doped TiO_2 photocatalysts samples were observed. This indicates that doped Ag and N in TiO_2 are well dispersed into TiO_2 as solid solution.

Average crystallite size of as-synthesized photocatalysts were obtained using Scherer formula [18–20] :

$$D = K\lambda/(\beta \cos\theta) \quad (1)$$

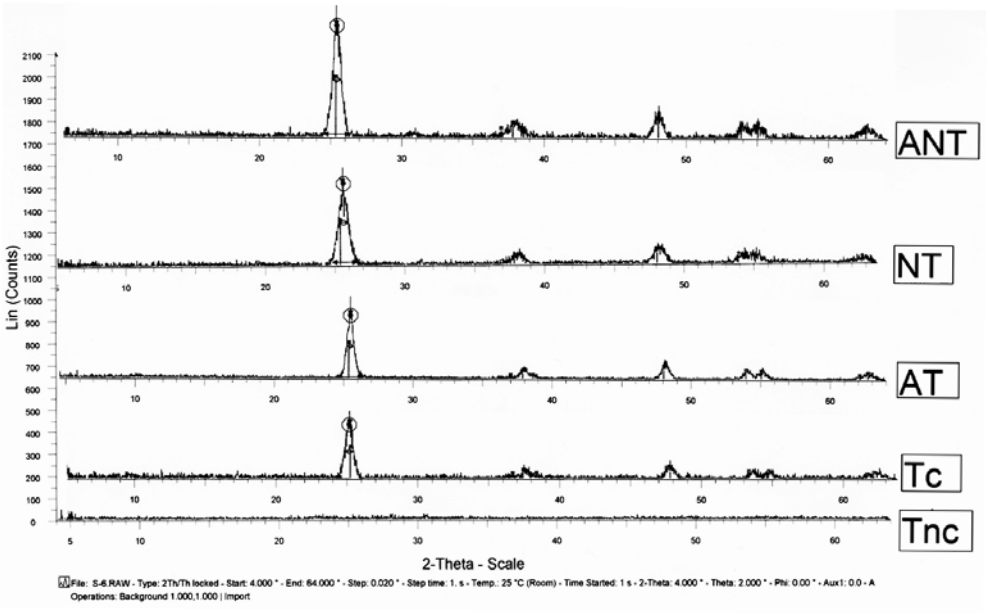

Fig. 1. XRD patterns of as-synthesized photocatalysts (Tnc = noncalcined TiO_2; Tc = calcined TiO_2; AT = Ag-doped TiO_2; NT = N-doped TiO_2 and ANT = Ag-N co-doped TiO_2).

Where, D = crystallite size in nm; K = shape factor constant, usually taken as 0.9; β = full width at half maximum (FWHM) in radians; λ = wave length of the X-ray (0.15406 nm) for Cu target Kα radiation and θ = Bragg's angle. The calculated higher crystallite size of Ag-doped TiO_2 than TiO_2 (Table-2) indicates the deposition of silver at TiO_2 surface. Lower particle size of N-doped TiO_2 compared to undoped TiO_2 suggest that doped N atoms either occupy the vacant lattice sites or replace oxygen atoms in the lattice.

TABLE 2.

Crystallite size of synthesized photocatalysts

Sample	2θ(degree)	B(degree)	D(nm)
T_c	25.140	0.629	12.94
AT	25.459	0.533	15.27
NT	25.556	0.724	11.25
ANT	25.345	0.661	12.32

(Tc = calcined TiO_2; AT = Ag-doped TiO_2; NT = N-doped TiO_2 and ANT = Ag-N co-doped TiO_2)

TEM Analysis :

TEM image of Ag-N co-doped TiO_2 photocatalyst powder is presented in Fig. 2. The observed average crystallite size, 24 nm, is higher than the corresponding value obtained by using Scherer formula, described in section 3.1. The observed TEM images of N-dope

UV/Visible absorbance study :

The optical absorbance spectra of the studied photocatalysts in the UV–Visible region are presented in Fig. 3. Absorption wave length (λ) values for calcined TiO_2, Ag-doped TiO_2, N-doped TiO_2 and Ag-N co-doped TiO_2 are : 395, 410, 485 and 505 nm, respectively. Band gap energy of as-synthesized photocatalyst samples were determined using the relation [19,21].

$$E_{bg}\ (eV) = 1240/\lambda \qquad (2)$$

Where, E_{bg} = band gap energy in electron volts, and λ = wave length at the intercept of the tangent line on the wave length axis. Band gap energies (E_{bg}) for calcined TiO_2, Ag-doped TiO_2, N-doped TiO_2 and Ag-N co-doped TiO_2 are : 3.14, 3.02, 2.56 and 2.45 eV, respectively. This clearly shows the synergetic effect of silver

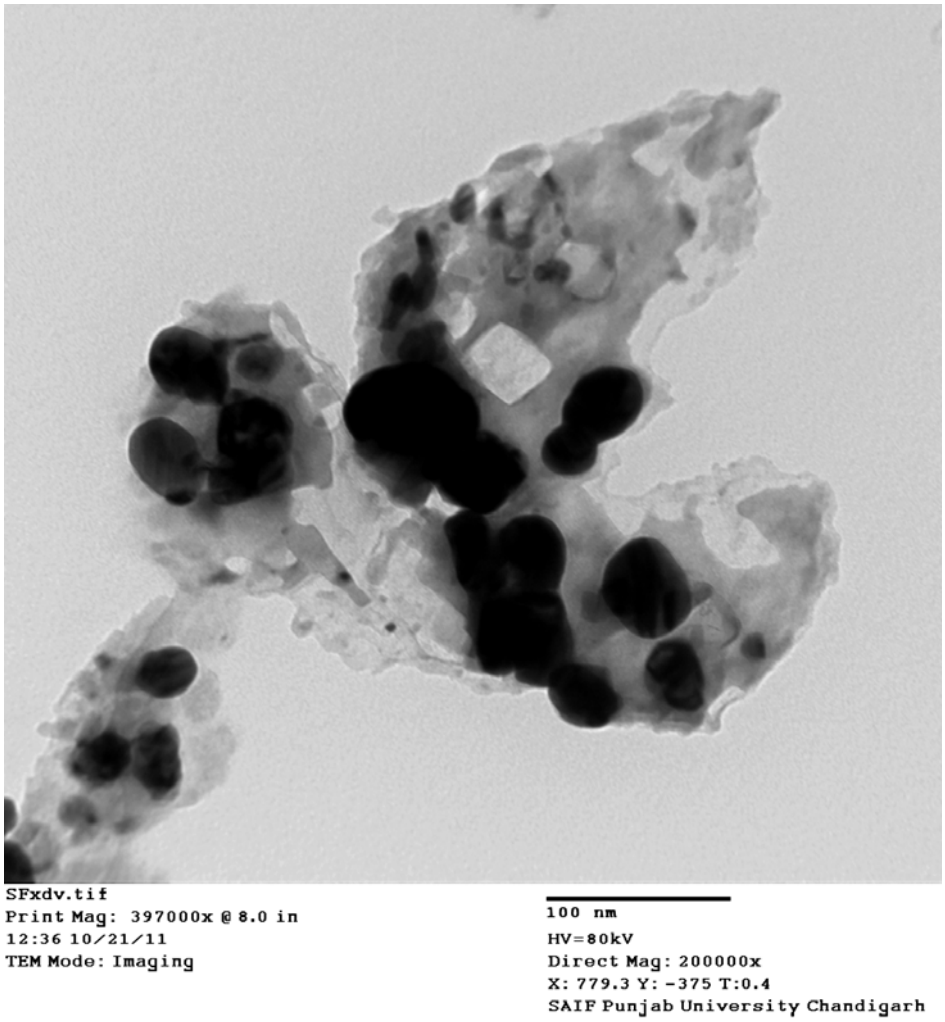

Fig. 2. TEM image of Ag-N co-doped TiO_2 photocatalyst powder.

and nitrogen co-doping in TiO_2 towards shifting of photo absorption edge towards visible light.

Photocatalytic degradation study :

In order to investigate the photocatalytic activity of the as-synthesized nanomaterial, degradation of methyl orange (MO) was carried out under UV and visible radiations.

The percentage degradation of MO was calculated using the equation [22]

$$\text{Degradation } (\%) = [(C_0 - C_t)/C_0] \times 100 \quad (3)$$

Where, C_0 = initial concentration of MO and C_t = concentration of MO at time 't' (in minutes). Percentage degradation of MO in aqueous solution as a function of time under UV and visible radiations are presented in Figs. 4 to 5, respectively. Percent degradation of methyl orange, at 120 minutes, using noncalcined TiO_2, calcined TiO_2,

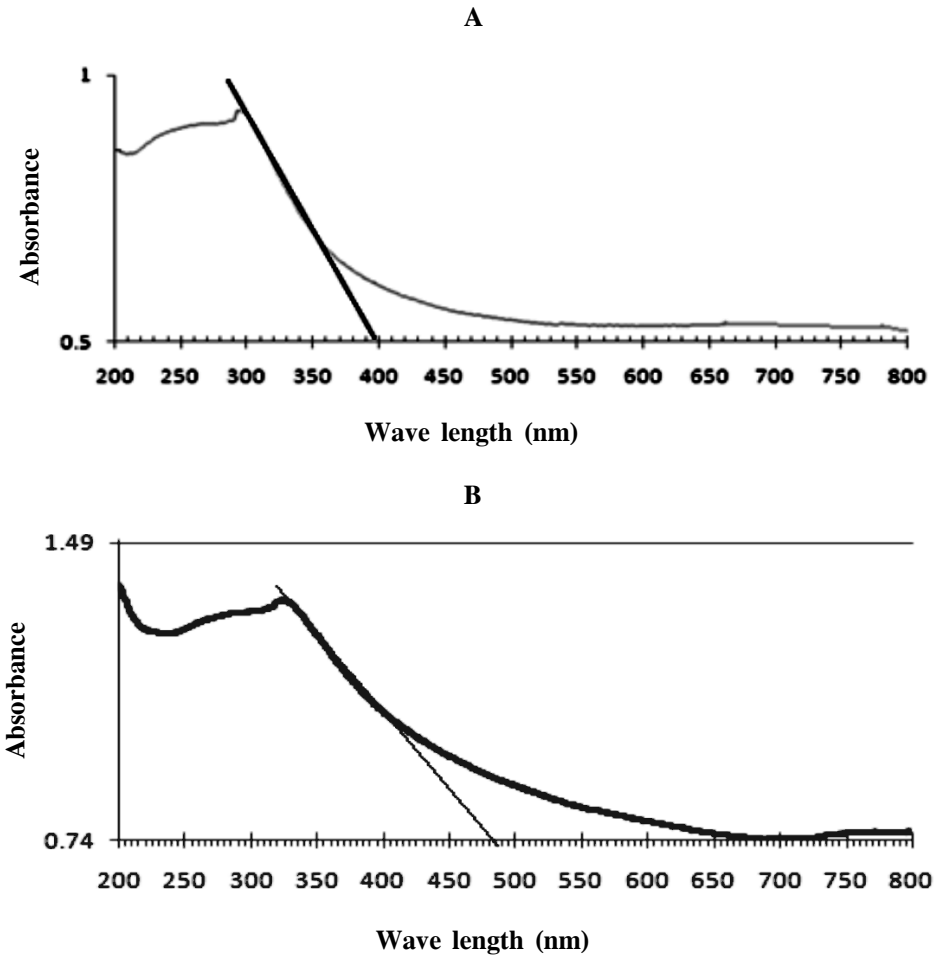

Fig. 3. Plots of absorbance as a function of wave-length (nm) and the observed UV/Visible absorption edge for as-synthesized photocatalyst samples : A : calcined TiO_2 (λ = 395); B : Ag-doped TiO_2(λ = 410 nm).

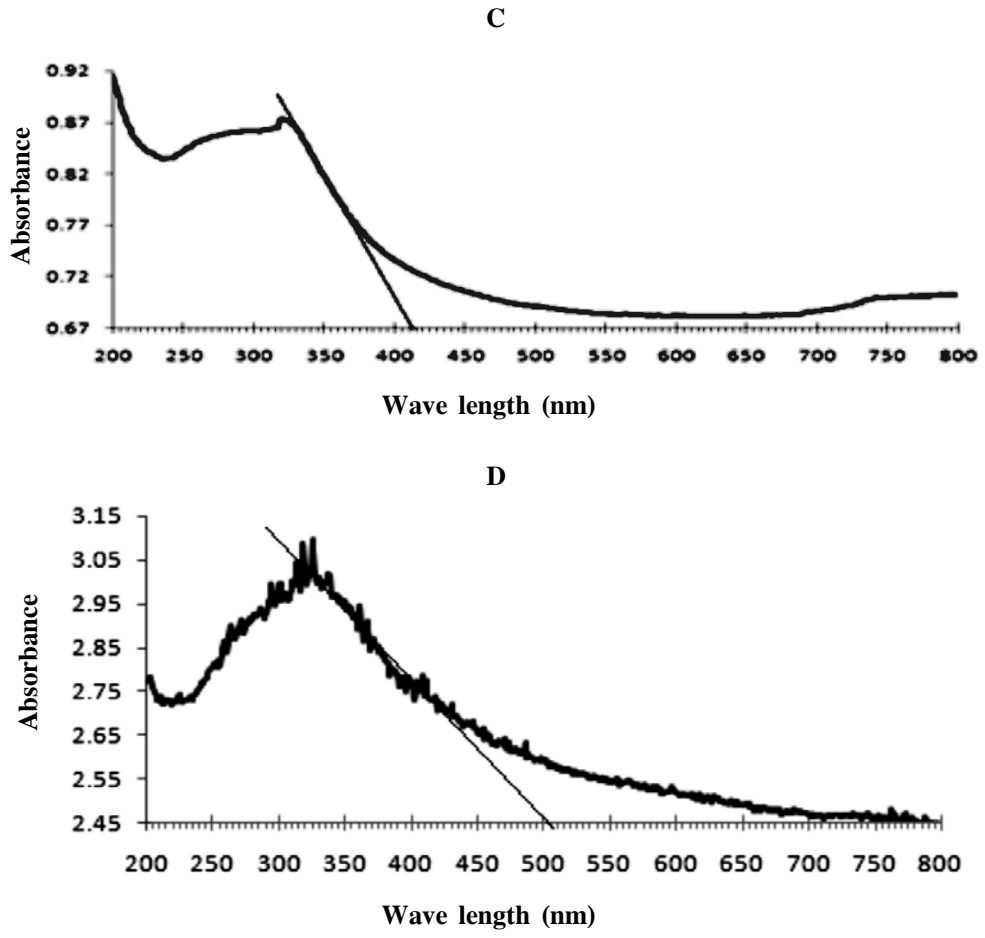

Fig. 3. Plots of absorbance as a function of wave-length (nm) and the observed UV/Visible absorption edge for as-synthesized photocatalyst samples : C : N-doped TiO_2 (λ = 485 nm) and D = Ag-N-co-doped TiO_2(λ = 505 nm).

Ag-doped TiO_2, N-doped TiO_2 and Ag-N co-doped TiO_2 : under UV irradiation were : 2.9, 16.0, 55.0, 40.2 and 79.1 respectively (Fig. 4.) and under visible light were 2.4, 11.9, 13.0, 26.2 and 73.00, respectively (Fig. 5).

Photocatalytic activity of uncalcined TiO_2 is much lower than for the remaining photocatalysts both under UV as well as visible irradiation. This may be due to non-bridging oxygen (NBO) in uncalcined amorphous phase of TiO_2, where defects in

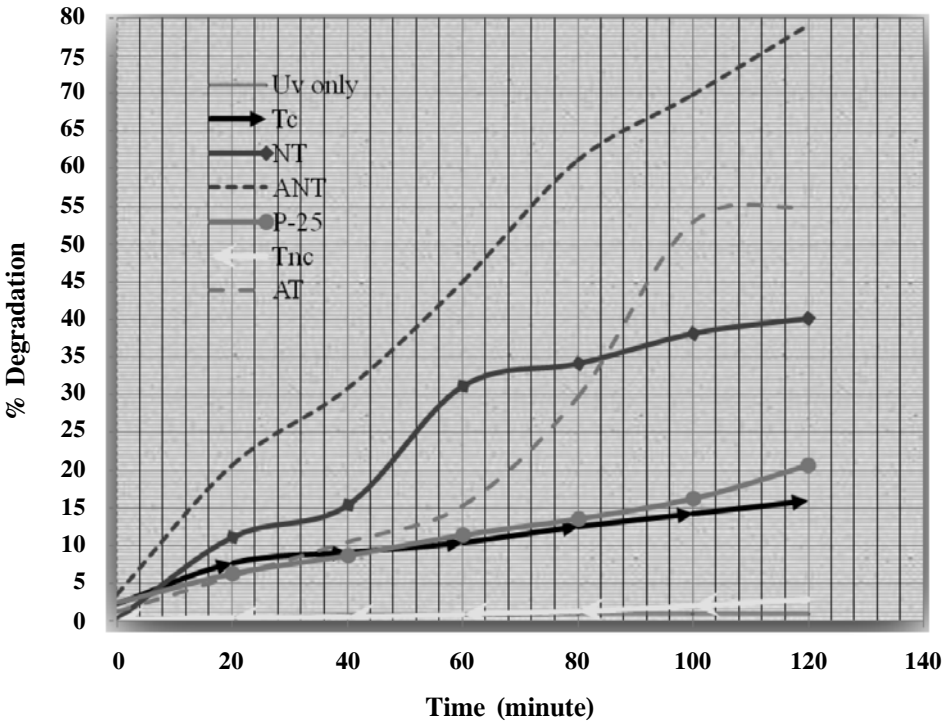

Fig. 4. Percent photocatalytic degradation of MO under UV irradiation using as-synthesized nanomaterial (Tc = calcined TiO_2; NT : N-doped TiO_2; ANT : Ag-N-co-doped TiO_2; P-25 : TiO_2(Degussa-25); Tnc : uncalcined TiO_2; AT : Ag-doped TiO_2).

Titanium and Oxygen atomic arrangement could facilitate recombination of photogenerated electron–hole pairs [23].

Photo-catalytic activity of Ag-N co-doped TiO_2 is higher than the remaining as-synthesized photo-catalysts or P-25 under both UV as well as visible irradiations. Under UV irradiation the percentage degradation of MO is higher using Ag-doped TiO_2 as photo-catalyst than under N-doped TiO_2 but the reverse is true under visible irradiation. Under UV irradiation, higher photo-catalytic activity of Ag-doped TiO_2 compared to N-doped TiO_2 may be due to entrapping of the photo-excited electrons by the doped silver, in the former photo-catalyst, thus inhibiting the recombination of electron-hole pairs [12,24]. Under visible radiation, photocatalytic activity of N-doped TiO_2 is higher compared to Ag-doped TiO_2. It is because doped N into TiO_2 modifies its electronic structure leading to the band gap narrowing [25] and thus enabling it to harvest more photons in the visible light [26–28].

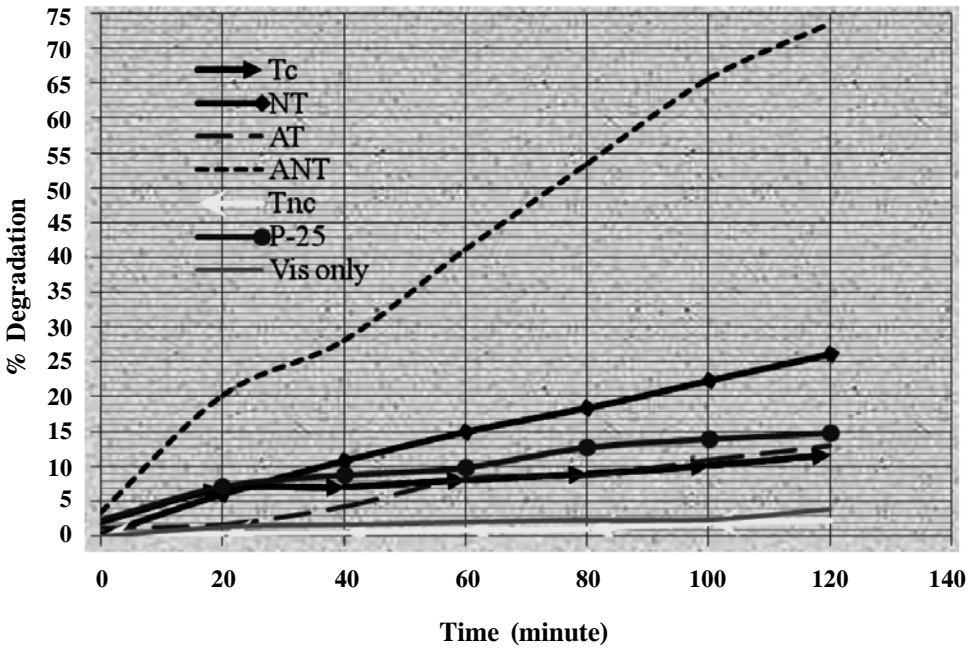

Fig. 5. Photocatalytic degradation of MO under visible irradiation using different as-synthesized nanomaterial (Tc = calcined TiO_2; NT : N-doped TiO_2; ANT : Ag-N-co-doped TiO_2; P-25 : TiO_2(Degussa-25); Tnc : uncalcined TiO_2; AT : Ag-doped TiO_2).

Mechanism of synergetic effect of Ag-N co-doping on photo-catalytalysis :

The proposed mechanism of synergetic effect of Ag-N co-doping in TiO_2 on the photocatalytic degradation of MO has been described in Fig. 6. Photocatalysis under UV irradiation, involves excitation of electrons from the valence band (VB) to the conduction band (CB) of TiO_2. The excited electrons are trapped by Ag^+ ion to form Ag^0 since the CB is at a lower reduction potential (–0.32 eV) compared to Ag^+ ion reduction potential (0.8 eV). Neutral Ag^0 atoms thus formed are then oxidized to their original state (Ag^+) with simultaneous conversion of adsorbed O_2 to superoxide ($O^{2\,\bullet-}$) radicals[12]. In this way, the recombination of photo-generated electrons and holes is minimized. In the subsequent steps, superoxide radicals formed, generate hydroxyl ($OH^\bullet$) radicals by combining with H_2O or OH^- ions. $OH^\bullet$ radicals which are highly oxidizing agents, degrade the substrate (methyl orange in the present case) molecules to non-toxic product, During photocatalysis under visible radiation, using N-doped TiO_2, excitation of electrons from VB of the photocatalyst to a newly

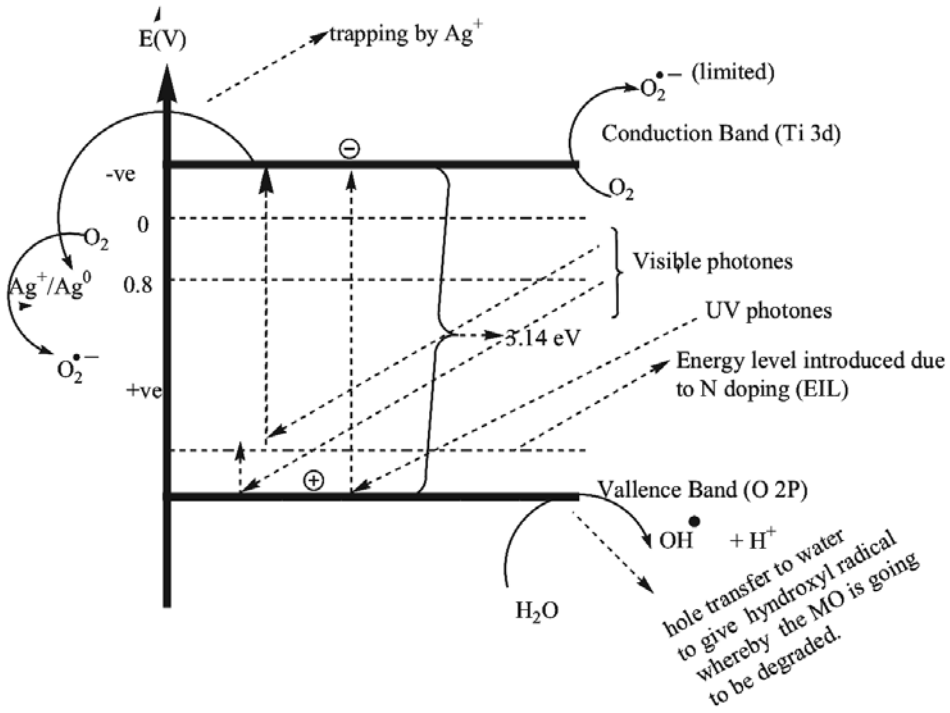

Fig. 6. Proposed mechanism of synergetic effect of Ag-N co-doping into TiO_2 on the photocatalytic degradation of methyl orange.

generated energy level (created by the doped nitrogen) takes place. It is followed by the absorption of new photons of visible radiation for the further transfer of electrons to the conduction band of TiO_2. The subsequent paths followed for the degradation of the substrate are similar as mentioned above in photocatalysis under UV radiation.

CONCLUSIONS

Synrgetically modified Ag-N co-doped anatase TiO_2 nanoparticles have been synthesized from $TiCl_4$ precursor. Incorporation of nitrogen into TiO_2 modifies its electronic properties extending its absorption edge to visible region of radiation. This is reflected in the observed enhanced photocatalytic-degradation of methyl orange under visible irradiation. Ag-doping in TiO_2 also shows a positive influence on its photocatalytic activity in the degradation of methyl orange under UV/visible irradiation over un-doped TiO_2. It is attributed to the electron-trapping ability of silver which

facilitates electron-hole-pair separation in TiO_2 semiconductor. Using Ag-N-co-doped TiO_2 as photocatalyst, percentage degradation of methyl orange at 120 minutes under UV and Visible radiation were 79.1% and 73.5%, respectively.

REFERENCES

1. M. D. Roldan, R. Blasco, F. J. Caballero, F. Castillo, *Arch. Microbiol*, 169, 36 (1998).
2. V. Meyer, *Water Sci. Technol.,* 26, 1205 (1992).
3. W. G. Kuo, *Water Res.*, 26, 881 (1992),
4. S. H. Lin and C. F. Peng, *Water Res.,* 28, 277 (1994).
5. M. Dogan and M. Alkan, *Chemosphere*, 50, 517 (2003).
6. B. Acemioglu, *J. Colloid and Interface Science*, 274, 371 (2004).
7. S. Arivoli, M. Sundaravadivelu and K. P. Elango, *Indian J. Chem. Tecnol.*, 15, 130 (2008).
8. K. Pelentridou. E. Stathatos, H. Karasali, D. D. Dionysiou and P. Lianos, Journal of Photoenergy, Hindawi Publishing Corporation Article, *ID 978329, doi:10.1155/2008/978329* (2008).
9. J. A. Anderson and M. F. Garcýa, *Catalysis*, 21, 51 (2009).
10. N. Modirshahla, B. M. Ali, J. Oskui and M. Reza, *Iran. J. Chem. Chem. Eng.,* 28, 49 (2009).
11. N. M. Esfahani and M. H. Habibi, *Desalination and Water Treatment*, 3, 64 (2009).
12. Z. He, L. Xie, S. Song, C. Wang, J. Tu and F. Hong,. *Journal of Molecular Catalysis A : Chemical* 319, 78 (2010).
13. A. Radwan and Al-Rasheed, *Water treatment by heterogeneous photocatalysis -A overview*. Presented in 4th Saline Water Desalination Research Institute Saline Water Conversion Corporation (SWCC) Symposium (2005).
14. A. Mills and S. LeHunte. *An overview of semiconductor photocatalysis*. Journal of Photochemistry and Photobiology. *A 108((*1997)*):1-35.* : In Radwan A. Al-Rasheed, 2005. *Water treatment by heterogeneous photocatalysis an overview*. Presented in 4th Saline Water Desalination Research Institute Saline Water Conversion Corporation (SWCC) Symposium.
15. G. S. Shephard, S. Stockenstrom, D.de Villiers, W. J. Engelbrecht, G. F. S Wessels, *Degradation of microcystin toxins in a falling film photocatalytic reactor with immobilized titanium dioxide catalyst*. Water Research 36 (2002), 140-146 : In Radwan A. Al-Rasheed, 2005. *Water treatment by heterogeneous photocatalysis an overview*. Presented in 4th Saline Water Desalination Research InstituteSaline Water Conversion Corporation (SWCC) symposium.

16. D. F. Ollis, E. pellizzetti and N. Serpone, *Environ. Sci Technol.*, 25, 1523 (1991).
17. D. Maria, H. Alonso, F. Fresno, S. Suárez and J. M. Coronado, *J. Energy Environ. Sci.*, 2, 1231 (2009).
18. C. Oprea, V. Ciupina, G. Prodan, *Investigation of nanocrystals using tem micrographs and electron diffraction technique*. National Conference on Applied Physics, Galati, Romania, June 9–10 (2006).
19. H. Gao, J. Zhou, D. Dai, Y. Qu, *Chem. Eng. Technol.*, 32, 867 (2009).
20. N. Sasirekha, B. Rajesh and W. Chen, *Thin Solid Films*, 518, 43 (2009).
21. X. Yang, F. Ma, K. Li, Y. Guo, J. Hu, W. Li, M. Huo and Y. Guo, *Journal of Hazardous Materials*, 175, 429 (2010).
22. N. Venkatachalam, M. Palanichamy and V. Murugesan, *J .Mol. Catal. A : Chemical.,* 273, 177 (2007).
23. Y. Xie and C. Yuan, *J. Chem. Technol. Biotechnol*, 80, 954 (2005).
24. Z. X. Shen, J. Guo, Z. Liu and S. Xie, *Applied Surface Science,* 254, 4726 (2008).
25. S. Rehman, R. Ullah, A. M. Butt and N. D. Gohar, *Journal of Hazardous Materials,* 170, 560 (2009).
26. J. Yuan, M. Chen, J. Shi and W. Shangguan, *International Journal of Hydrogen Energy*, 31, 1326 (2006).
27. H. Shen, L. Mi, P. Xu, W. Shen and P. N. Wang, *Applied Surface Science*, 253, 7024 (2007).
28. Y. Yin, W. Zhang, S. Chen and S. Yua, *Materials Chemistry and Physics*, 113, 982 (2009).
29. X. Yang, F. Ma, K. Li, Y. Guo, J. Hu, W. Li, M. Huo and Y. Guo, *Journal of Hazardous Materials*, 175, 429 (2010).